Vietnam Journal of Science and Technology
DOI: https://doi.org/10.15625/2525-2518/22015

Biomechanical impact analysis of implant positioning in lumbar interbody fusion by the finite element method

Le Duy Nguyen Ho[1,3], Thi Hoang Thuy Le[1,3], Thuc Tri Dang[2,3], Truc Tam Vu[4], Thien Tich Truong[2,3,*]

[1]*Department of Biomedical Engineering, Faculty of Applied Science, Ho Chi Minh City University of Technology (HCMUT), 268 Ly Thuong Kiet street, Dien Hong ward, Ho Chi Minh City, Viet Nam*
[2]*Department of Engineering Mechanics, Faculty of Applied Science, Ho Chi Minh City University of Technology (HCMUT), 268 Ly Thuong Kiet street, Dien Hong ward, Ho Chi Minh City, Viet Nam*
[3]*Vietnam National University Ho Chi Minh City, Vo Truong Toan street, VNU-HCM Urban Area, Quarter 33, Linh Xuan ward, Ho Chi Minh City, Viet Nam*
[4]*Department of Spinal Surgery B, Hospital for Traumatology and Orthopedics, 929 Tran Hung Dao street, Cho Quan ward, Ho Chi Minh City, Viet Nam*

[*]Email: *tttruong@hcmut.edu.vn*

Received: 29 November 2024; Accepted for publication: 07 May 2025

Abstract. Transforaminal Lumbar Interbody Fusion (TLIF) is a fusion technique in spinal surgeries reserved for chronic conditions requiring stabilization e.g. lumbar spinal stenosis and spondylolisthesis, especially when conservative treatments fail. The procedure involves removing the pathological disc material and putting a spacer with morselized bone graft in the disc space via the transforaminal pathway in order to promote interbody bony fusion. The whole construction is stabilized posteriorly by pedicle screw fixation. However, the conventional TLIF technique possessed several drawbacks including cage subsidence and cage protrusion, due to the posterior position of the cage within the disc space and modifications have been proposed in the effort to reduce the mentioned problems. Selecting pedicle screw length is also a topic to debate, when no clear consensus has been established regarding that matter. Therefore, this study uses Finite Element (FE) model under physiological axial compression to investigate the screw length and cage positioning effects on the bone and instruments. This model accounts for the structural interactions between the cage, pedicle screws, and surrounding bone tissue. Our findings highlight the novel insight that anterior cage placement reduces the risk of cage subsidence and improves load distribution. Additionally, the study demonstrates that screw tips should extend beyond the center of the cage to enhance load transfer efficiency and reduce stress on the fixation system.

Keywords: finite element model, transforaminal lumbar interbody fusion, biomechanical stability, cage positioning.

Classification numbers: 2.7.1, 5.4.3.

1. INTRODUCTION

Spinal instrumentation and fusion techniques including Transforaminal Lumbar Interbody Fusion (TLIF) have a broad spectrum of indications, from severe unstable spinal stenosis to spondylolisthesis and degenerative spinal deformity. Despite the fact that Anterior Lumbar Interbody Fusion (ALIF) and Oblique Lumbar Interbody Fusion (OLIF) with or without posterior instrumentation are becoming increasingly popular, all posterior operations such as TLIF remain the first-line-option for most surgeons, especially in developing countries like Vietnam, thanks to its familiarity and less equipment-demanding than the aforementioned surgeries. In traditional TLIF technique, after disc preparation, morselized bone graft was inserted into the disc space and then the cage. The cage location in the posterior half of the disc space is thought to be the cause of complications e.g. cage protrusion and subsidence. Recent studies [1-3] have shown that inserting the cage to the anterior half of the disc space can reduce the risk of cage subsidence and protrusion. Another important consideration is determining the appropriate length of the pedicle screw in a given scenario. With advancements in computational modeling, finite element analysis has emerged as a powerful tool to investigate the biomechanical behavior of various surgical configurations, such as TLIF and ALIF. This study uses finite element models to analyze the biomechanical impact of screw length and interbody cage position in TLIF surgery, incorporating pedicle screws, interbody cage, and vertebral bone derived from Computational Tomography (CT) scan data of Vietnamese patients. The models represent the lumbar spine segment L4/5 with the banana-shaped PolyEther Ether Ketone (PEEK) cage and titanium pedicle screws positioned within the disc space, simulating different cage placements and screw lengths to evaluate their biomechanical effects. Axial loads are applied to the model to simulate real-world spinal loading conditions, calculating stress, strain, and deformation to assess the impact of cage position and screw length on spinal stability.

2. MATERIALS AND METHODS

2.1. Building a validated model

The experimental model from the literature [4] was simulated to validate the finite element method by comparing the strain results. A single-level synthetic spine model includes two Ultra-High-Molecular-Weight Polyethylene (UHMWPe) cylinders, four stainless steel pedicle screws (7 mm diameter, 40 mm length), and two 5-mm rods. The single large oval titanium cage (28 mm × 35 mm, 18 mm height) was positioned anteriorly, corresponding to group 3 in the literature. Detailed material parameters are displayed in Table 1, including elastic Young's modulus and Poisson's ratio. The model was drawn in SolidWorks based on the design of the paper and then was imported into ANSYS for discretizing into the combination of tetrahedral elements for cylinders, screws and hexahedral elements for the rods and cage (Figure 1). Element size of 1 mm was used for the whole model. The load of 600 N was applied to the superior endplate of the upper cylinder, and the inferior endplate of the lower cylinder was fixed.

Table 1. Mechanical parameters of the validated model.

Component	Young's modulus (MPa)	Poisson's ratio	Ref.
Titanium	110,000	0.35	[5]

Stainless steel	190,000	0.275	[6]
UHMWPe	450	0.4	[7]

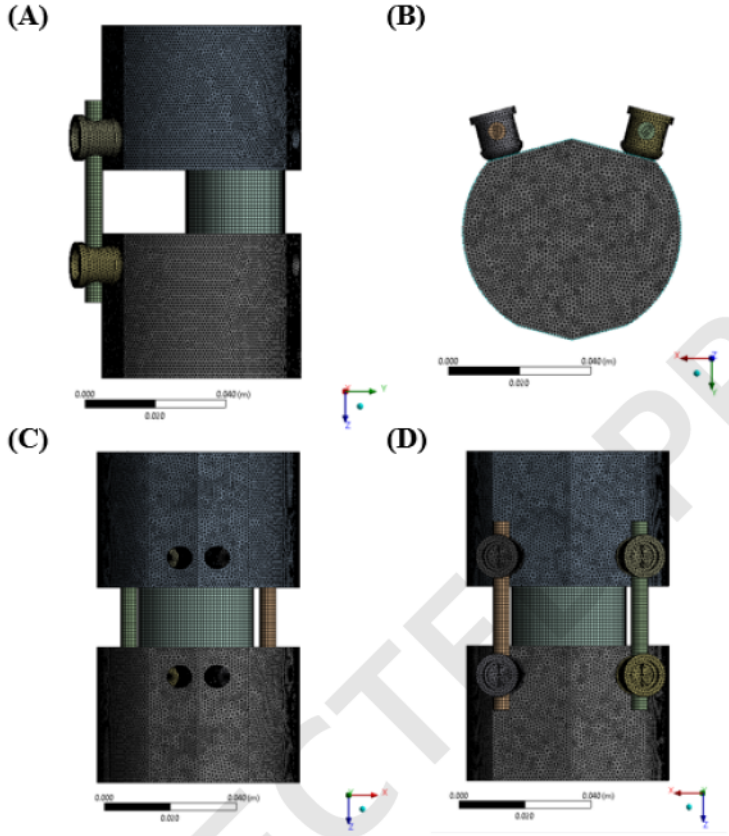

Figure 1. Three-dimensional FE model of the validated model observed from side view (A), top view (B), front view (C), and back view (D).

2.2. Construction of TLIF configurations

2.2.1. Building three-dimensional model from CT scan

The TLIF surgical method involves a sequence of steps aimed at stabilizing the spine in cases of degenerative disc disease, spondylolisthesis, or other spinal deformities. Initially, the surgeon accesses the spine through a posterior incision. After exposing the affected vertebrae, the intervertebral disc is removed, and a morselized bone graft is inserted into the disc space to promote fusion. A PEEK cage is placed in the intervertebral space to maintain disc height and support the fusion process. The cage is designed with a banana shape to fit the natural curvature of the spine. Pedicle screws, typically made from titanium, are then inserted into the vertebrae. These screws anchor a titanium rod that connects them, providing stability and immobilizing the fused segment. The titanium screws and rod work together to maintain the alignment of the vertebrae, while the PEEK cage allows for proper healing and fusion. This procedure, when performed correctly, helps alleviate pain and restore spinal stability. The PEEK cage material is chosen for its biocompatibility, while the titanium screws and rod ensure strong, durable fixation throughout the healing process.

The advantages of TLIF include strong spinal stabilization, reduced risk of cage subsidence due to the firm fixation system including rods and screws, which promotes fusion and biocompatibility. The posterior approach also offers smaller incisions, reducing recovery time and minimizing nerve damage. However, the disadvantages include risks of nerve root injury and hardware failure if screws or the cage are mispositioned. The posterior approach can also limit visualization of the disc space, and patients may require extensive postoperative care to ensure proper healing and fusion.

In this study, the TLIF models were constructed to address two critical biomechanical challenges in spinal fusion surgery. The first problem focuses on assessing pedicle screw length, specifically insufficient screw proximity to posterior vertebral elements and the failure of screw tips to extend beyond the cage when viewed in the sagittal plane. The second problem examines the influence of cage positioning – anterior versus posterior – on the biomechanical performance of the fused segment when screws are correctly positioned.

To ensure the study effectively addresses these challenges, the L4-L5 segment was selected as the focus for modeling intervertebral fusion surgery, given its susceptibility to degeneration and its clinical relevance in TLIF procedures. A nonlinear three-dimensional FE model of the L4-L5 spinal segment was developed in ANSYS Student Version 2024 from CT data of a 32-year-old woman's lumbar spine. The donor was recorded with no bone abnormalities at unit L4-L5. The protocol in the flow chart (Figure 2) summarizes the process of constructing the FE model from sample data.

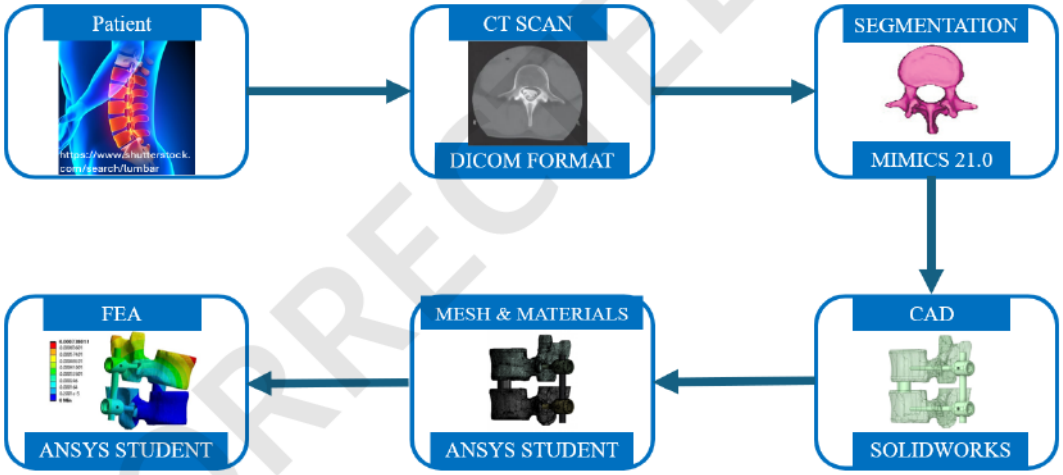

Figure 2. The process of L4-L5 FE model construction from CT data for simulation [8].

By using Mimics 21.0 software, the CT images in Digital Imaging and COmmunications in Medicine (DICOM) format were segmented. To derive detailed surfaces in accordance with the bony structures of L4-L5, automatic segmentation was implemented upon thresholding of the CT grayscale values, whilst hand-executed segmentation was performed in sections of the images slice by slice. The binary stl files were generated from Mimics 21.0, then were imported into SolidWorks, a tool using point cloud data to develop Non-Uniform Rational B-spline (NURB) surfaces recorded as stp ap203 files. To produce discrete solid pieces for the L4 and L5 bones, we imported those stp files into ANSYS Workbench. Those surfaces were subsequently meshed and discretized into tetrahedral elements for the bony structures and fixation implants.

Regarding the implants fixed into the TLIF constructs, the cage is made of PolyEther Ether Ketone (PEEK), four pedicle screws and two connecting rods are made of titanium. The cage inserted into L4-L5 disc space has banana shape and parameters of 10 mm height, 11.5 mm width, and 26 mm length (Figure 3). The rod measures 100 mm in length and has a diameter of 9.64 mm. The screw parameters vary depending on the specific case and will be detailed accordingly for each scenario.

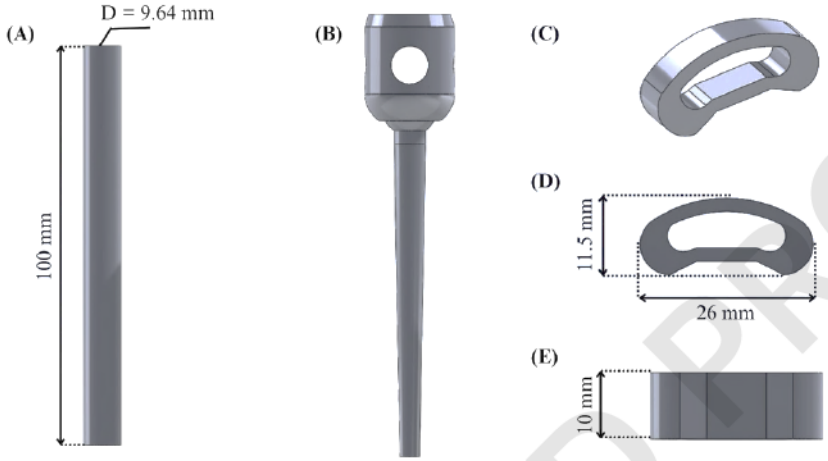

Figure 3. Implant components of the designed fixation system: connecting rod (A), pedicle screw (B), and cage (C) with its dimensions (D, E).

In terms of material assignments, the fixation system was constructed in which the multiple materials were defined to be homogeneous. The material parameters were set comprising of cancellous bone, interbody fusion cage, posterior screws and rods, all of which were applied to distinct elastic Young's modulus and Poisson's ratio [9, 10]. Figure 4 illustrates the material type assigned for each implant in the fixation system and describes their roles. Table 2 illustrates the varieties of material parameters for each component of the TLIF model.

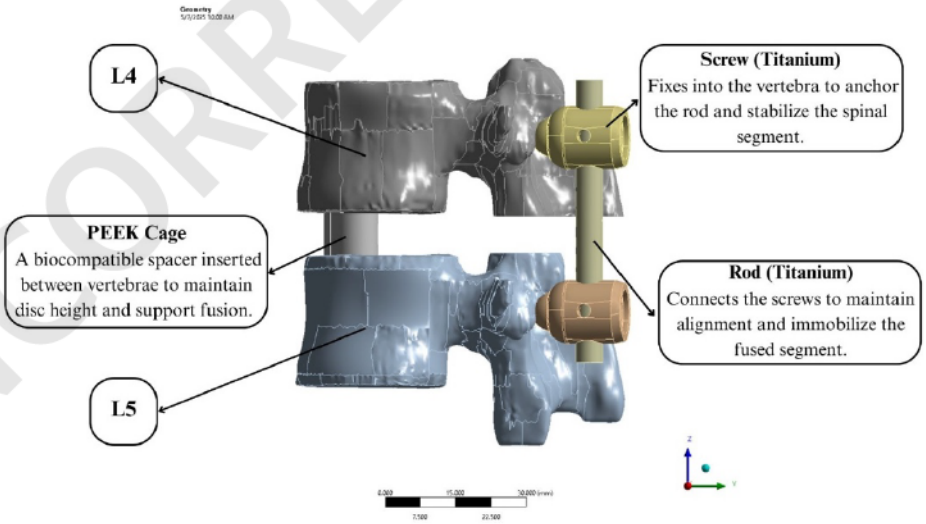

Figure 4. Illustration of TLIF construct with PEEK cage, titanium pedicle screws and rods for spinal stabilization.

Table 2. Mechanical parameters of the implanted L4-L5 model.

Component	Young's modulus (MPa)	Poisson's ratio	Ref.
Cancellous bone	320	0.2	[11, 12]
PEEK	3,500	0.35	[13]
Titanium	110,000	0.35	[5]

To simulate physiological conditions, a vertical load of 500 N, representing body weight, was applied to the top of the L4 vertebra, with L5 inferior fixed as a stationary base. As shown in Figure 5, the compressive force of 500 N was applied at region (A), which corresponds to the superior surface of the L4 vertebra, while the inferior surface of L5 was fully constrained at region (B).

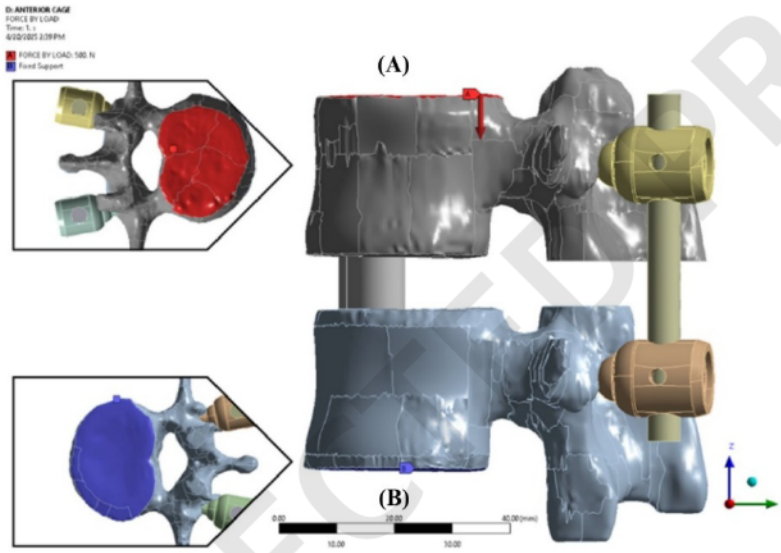

Figure 5. Boundary conditions and load application at L4 superior endplate (A) and L5 inferior endplate (B).

The screw-bone interface was assumed to be a bonded contact. The primary function of pedicle screws in spinal fusion is to provide rigid fixation, therefore, the screw and the surrounding bone were treated as a unified structure. Bonded type was also applied on the interface of screw-rod and bone-cage. The bending moment of 10 Nm was applied to the upper endplate of L4 to perform one of the common anatomical activities of the lumbar spine – FLexion (FL). The equivalent von-Mises stresses were observed within the fixation system, including the lower endplate of vertebrae L4, upper endplate of vertebrae L5, fusion cage, and two posterior connecting rods, providing insights into the mechanical performance of the construct.

2.2.2. Analyzing pedicle screw length

To address the first problem, two screw configurations were simulated to evaluate the impact of screw length on biomechanical performance. The first configuration (Case 1) employed long screw length, with screw tips extending beyond the cage's center to enhance load transfer efficiency. The pedicle screw in this case has an overall length of 49.93 mm, a head diameter of 4.78 mm, and a tip diameter of 3.02 mm. While the second configuration (Case 2) involved short screw length, where the screw tips did not extend beyond the interbody

cage in the sagittal plane, and screw placement is inadequate relative to the posterior vertebral elements (Figure 6). For Case 2, the pedicle screw features a reduced overall length of 43.96 mm, a head diameter of 4.78 mm, and a tip diameter of 3.20 mm.

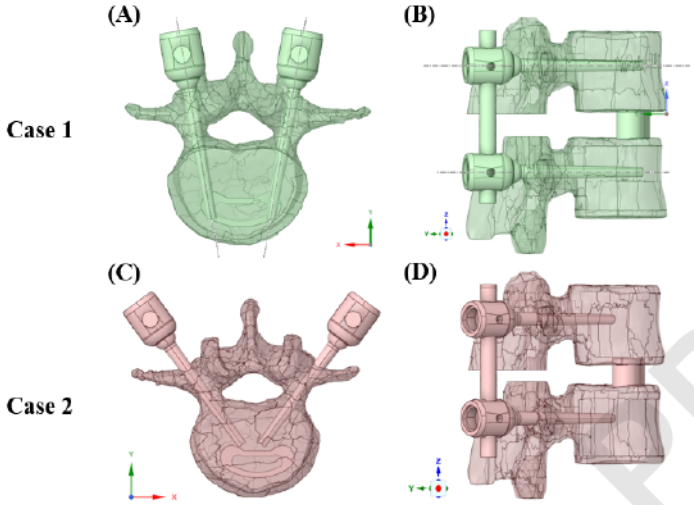

Figure 6. Three-dimensional model of Case 1 (A-B) and Case 2 (C-D).

2.2.3. Comparing anterior and posterior cage positioning

For the second problem, after establishing the suitable screw configuration, the influence of cage positioning was investigated by varying cage along the sagittal axis in two surgically relevant positions: Anterior Position (AP) and Posterior Position (PP) (Figure 7). In AP, the posterior edge of the cage aligns with the longitudinal axis of the vertebral body. In PP, the cage was placed 5 mm from the posterior edge of the L5 vertebrae. The pedicle screw parameters for this case are identical to Case 1 of the first problem, with an overall length of 49.93 mm, a head diameter of 4.78 mm, and a tip diameter of 3.02 mm.

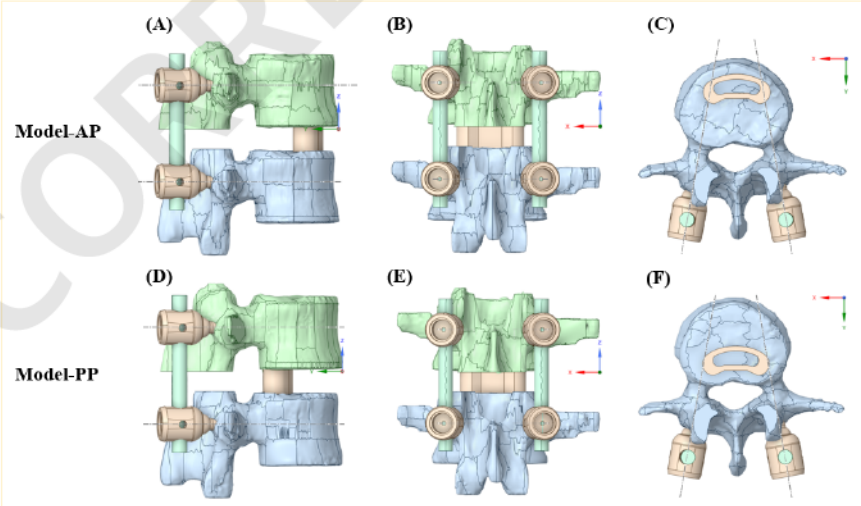

Figure 7. Three-dimensional model of anterior fusion cage placement (A-C) and posterior fusion cage placement (D-F).

The simulations were conducted in a sequential manner. First, the effect of pedicle screw length was analyzed by comparing the biomechanical performance of short versus suitably long pedicle screw dimensions using the anterior cage placement model. Next, the impact of cage positioning was assessed by comparing anterior and posterior cage placement models, ensuring the screw tips extended beyond the cage's center. This systematic approach enabled a comprehensive evaluation of the roles of pedicle fixation screw length and cage positioning in assessing the biomechanical performance of TLIF constructs.

3. RESULTS AND DISCUSSION

3.1. Model validity and Mesh convergence verification

3.1.1. Model validity

The strains of cage and rods in the simulated model were compared with the previously published study of Polly *et al.* after applying the same 600 N load as described in the literature [4]. The strain results of our validated FE model compared to the experimental model are 181.78 vs. 203 mm/mm for the rod and 137.96 vs. 140 mm/mm for the cage. The differences between these results are approximately 10 % for the rod and 1.5 % for the cage, as illustrated in Figure 8. This confirms the effectiveness of the method employed in this study.

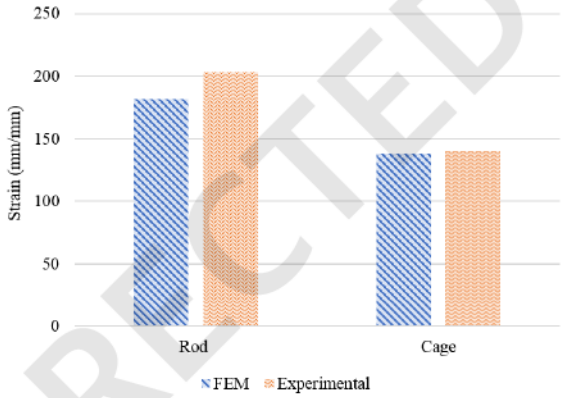

Figure 8. Comparison of strain between the FE model and experimental data of Polly *et al.* [4].

3.1.2. Mesh convergence verification

The maximum total deformation and maximum equivalent von-Mises stress results of cage in FE model of L4-L5 fixation system were analyzed in four element sizes: 1 mm, 1.5 mm, 2 mm, and 2.5 mm to verify the convergence of the mesh of TLIF constructs (Table 3). The resolution difference between the results of the 1.5 mm mesh size and the 1.0 mm mesh size was considered convergent, as shown in the line chart (Figure 9). Therefore, the 1.5 mm mesh size was chosen for the FE model.

Table 3. Mesh sensitivity analysis: Equivalent stress and total deformation.

Element size (mm)	Equivalent stress (MPa)	Total deformation (mm)
1.0	3.1809	0.0719

1.5	3.2273	0.0719
2.0	3.2862	0.0720
2.5	3.3169	0.0721

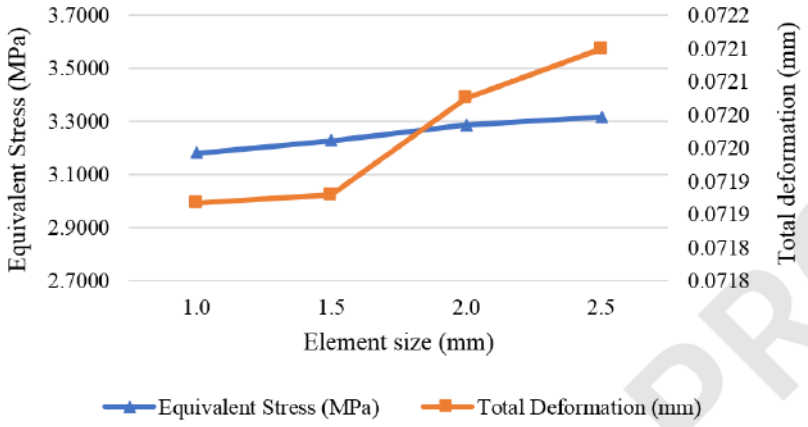

Figure 9. Result of meshing sensitivity study.

3.2. Analyzing pedicle screw length

The peak stresses experienced by the intervertebral cage under neutral and flexion motions are presented in Figure 10A. The highest stress observed was 76.89 MPa in Case 1 during the neutral posture, which is 3.05 times greater than the corresponding value in Case 2 (25.24 MPa). Under flexion, the cage in Case 1 also exhibited slightly higher stress compared to Case 2, with values of 46.56 MPa and 44.81 MPa, respectively.

Figure 10B illustrates the maximum stress on the connecting rods. Under flexion, the rods in Case 2 experienced significantly greater stress than those in Case 1, with values of 186.67 MPa and 54.90 MPa, respectively. In contrast, during the neutral posture, the stress in Case 2 was marginally lower than in Case 1, measured at 53.15 MPa and 70.40 MPa, respectively. Notably, the stress variation between postures in Case 1 was only 15.50 MPa, whereas in Case 2, this difference was markedly larger at 133.52 MPa. These findings highlight differences in load distribution and stability between the two cases.

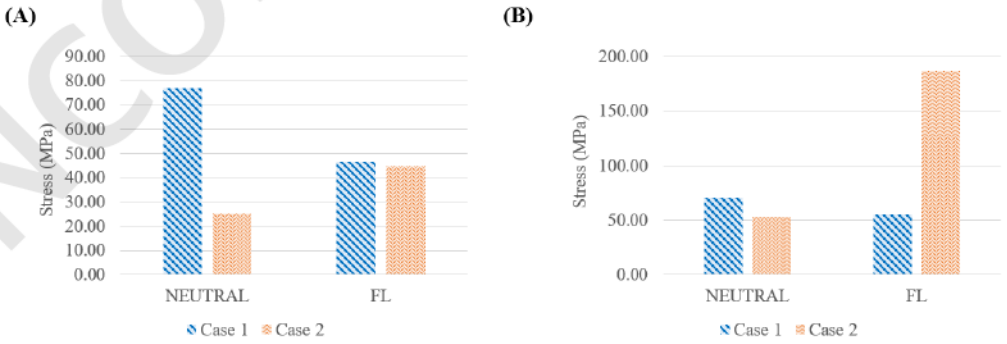

Figure 10. Comparison maximum equivalent (von-Mises) stress of the cage (A) and rod (B) between Case 1 and Case 2 during Neutral and FL postures.

3.3. Comparing anterior and posterior cage positioning

The von-Mises stress data presented in bar charts illustrate the differences between Anterior cage Placement (AP) and Posterior cage Placement (PP) models. Figure 11 compares the maximum stress on the connecting rod under two postures for the AP and PP models. The highest recorded stress was 119.93 MPa in the PP model during flexion, which was 2.18 times greater than the 54.90 MPa observed in the AP model under the same condition. Conversely, under the neutral posture, the maximum stress in the AP model exceeded that of the PP model, with values of 70.40 MPa and 19.15 MPa, respectively. Notably, the stress variation between postures was only 15.50 MPa in the AP model, compared to a substantially larger difference of 100.78 MPa in the PP model. These results underscore differences in the load-bearing capacity and mechanical stability of the rod between the two configurations.

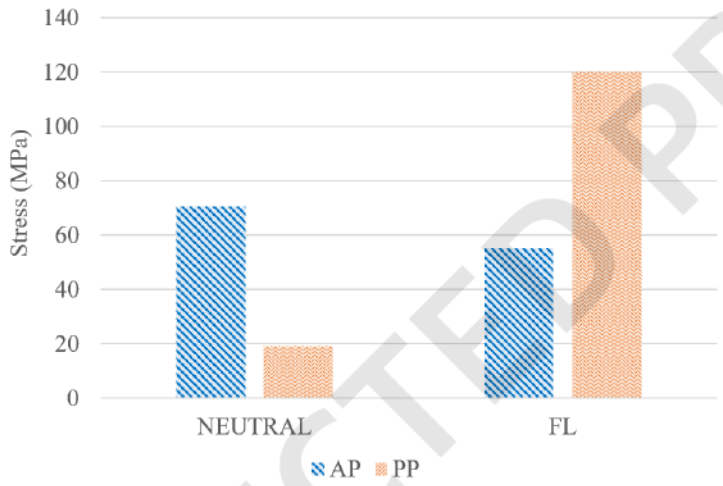

Figure 11. Peak von-Mises stress in the rod between AP and PP during Neutral and FL.

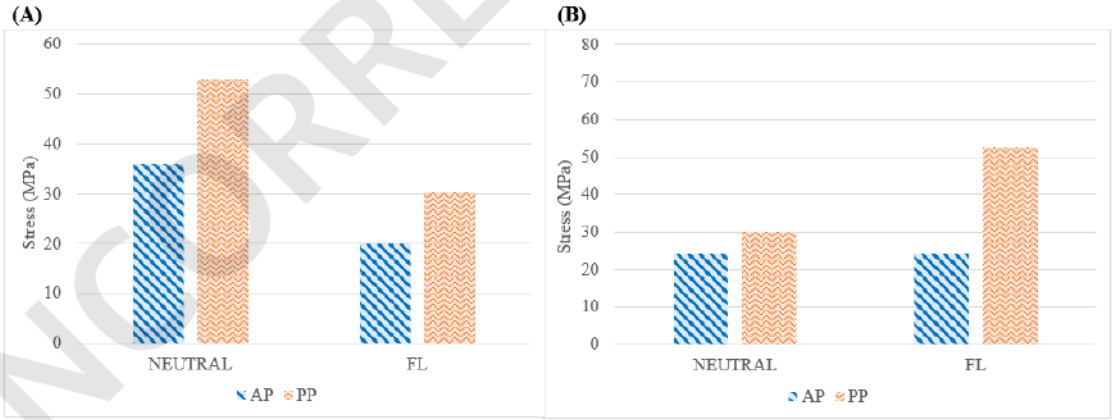

Figure 12. Maximum equivalent (von-Mises) stress of L4 lower endplate (A) and L5 upper endplate (B) between AP and PP during Neutral and FL.

Figure 12 illustrates the maximum von-Mises stress values at the L4 inferior endplate (Figure 12A) and the L5 superior endplate (Figure 12B) under both neutral and flexion (FL) conditions. For the L4 endplate, the AP model exhibited lower stress than the PP model in both

positions, with values of 36.077 MPa vs. 52.566 MPa in neutral and 20.240 MPa vs. 30.253 MPa in flexion, respectively. Similarly, for the L5 endplate, the AP configuration consistently maintained lower stress levels, remaining constant at 24.237 MPa across both conditions, while the PP model showed 30.215 MPa in neutral and increased significantly to 52.633 MPa in flexion. These findings confirm that AP effectively reduces stress on adjacent endplates, indicating a lower risk of mechanical failure and endplate subsidence compared to the PP, which demonstrated higher and less consistent stress levels across loading conditions.

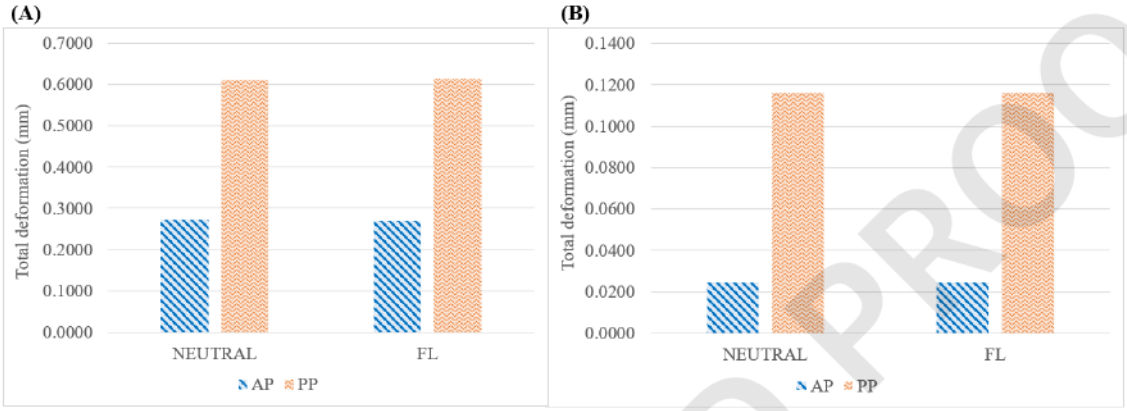

Figure 13. Total deformation of L4 lower endplate (A) and L5 upper endplate (B) between AP and PP during Neutral and FL.

Figure 13 presents the total deformation measurements of the L4 lower endplate (Figure 13A) and L5 upper endplate (Figure 13B). According to the values, the AP model again showed superior biomechanical stability with significantly lower deformation. At the L4 level, deformation in the AP model was 0.272 mm in neutral and 0.272 mm in flexion, whereas the PP model reached 0.612 mm and 0.613 mm, respectively. At the L5 level, AP deformation remained minimal and constant at 0.0246 mm under both loading conditions. In contrast, the PP model showed markedly higher deformation values of 0.116 mm for both neutral and flexion. This consistent difference highlights the AP model's improved ability to maintain structural integrity under mechanical loading, whereas the PP model presents a higher deformation response, which could contribute to long-term instability or implant migration.

Figures 14 and 15 present the von-Mises stress nephograms of the L4 inferior and L5 superior endplates, respectively, under neutral and flexion conditions. In both figures, peak stress is clearly concentrated at the cage-endplate interface, which is the critical load-bearing region. While stress distributions are visible in both AP and PP models, the high-stress zones appear more defined and localized in the PP model. These visualizations further support the mechanical relevance of the endplate-cage contact area and highlight its importance in construct evaluation.

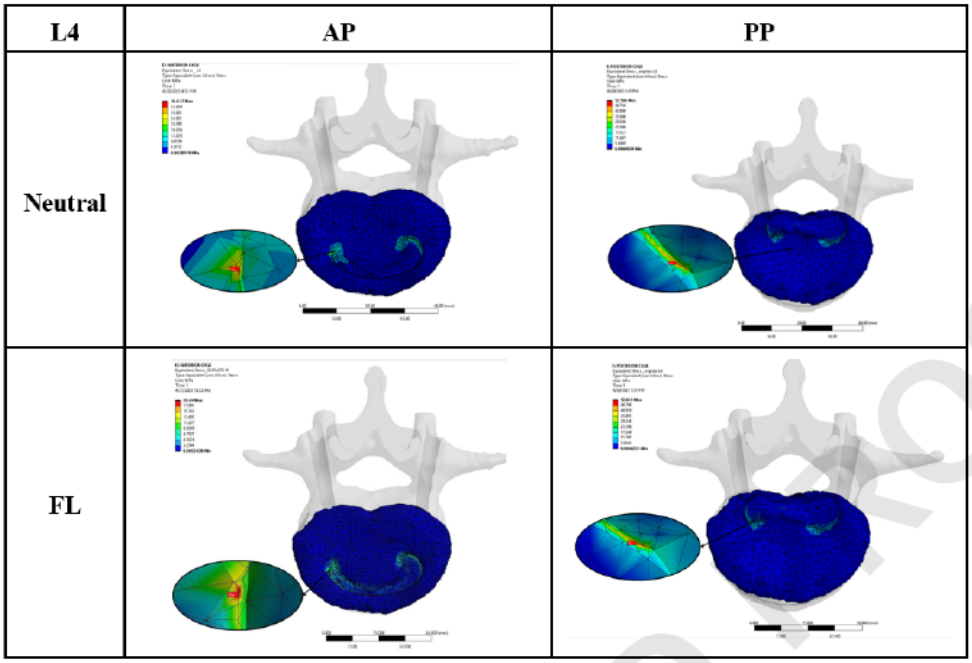

Figure 14. The stress nephogram of lower endplate L4 vertebra.

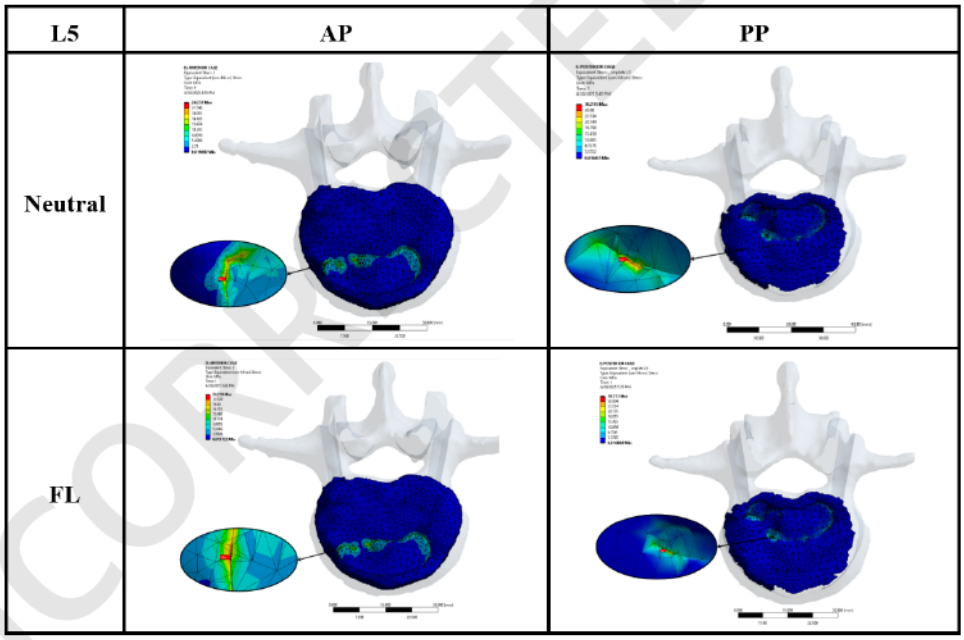

Figure 15. The stress nephogram of upper endplate L5 vertebra.

3.4. Discussion

For the first problem, higher stress values on the bone cage were observed in Case 1, where longer screws were implemented, in both neutral and flexion (FL) positions. This suggests that when the screw tips extended beyond the cage center, as viewed in the sagittal

plane, the cage was able to better absorb the axial load. This can be explained by the fact that the screw, fixed at one end, experiences a uniformly distributed load, with the bending moment being greatest at the fixed end and gradually decreasing towards the screw tip. When the screw tip does not extend beyond the center of the cage, the moment force exerted on the cage is minimal, as it is primarily influenced by the vertebral bone, leading to reduced load-bearing capacity of the cage.

Regarding the stress on the rod, in the flexion posture, the stress in Case 1 was significantly lower than in Case 2. In the neutral position, the stress on the rod was slightly higher in Case 1 which has the longer axial length of screws. However, within Case 1, the stress values did not vary greatly between the neutral and flexion positions. This suggests that the load-bearing capacity of the rod is more stable in Case 1 compared to Case 2, where the stress difference between the two postures was much larger. These findings indicate that when the screw tips reach beyond the fulcrum of the cage, the whole configuration will be improved in terms of load-bearing capacity of the cage and stress on the connecting rod.

The second investigation demonstrates that, in the flexion posture, the rod stress associated with anterior cage placement is significantly lower compared to posterior placement. This finding suggests that positioning the cage anteriorly effectively reduces the load borne by the rod during flexion, a posture frequently encountered in daily activities. In the neutral posture, although rod stress is lower in the posterior cage placement compared to the anterior placement, the difference in rod stress between neutral and flexion postures is minimal in the anterior configuration. This suggests that the distracting stress on the rods in the anterior setup exhibits great consistency, meanwhile a much larger stress variation can be observed in posterior configuration during posture change.

The von-Mises stress distribution and the total deformation outcomes on the L4 inferior and L5 superior endplates indicated that the anterior cage configuration consistently experienced lower peak stresses than the posterior cage in both neutral and flexion postures. These findings collectively indicate the biomechanical benefits of anterior cage positioning in mitigating the risk of cage subsidence and maintaining construct stability.

Overall, between the two positions of the cage, the anterior placement has superior biomechanical characteristics by reducing the compression stress on the connecting rod and the L4 inferior and L5 superior endplates. This configuration enhances the rod's durability, lowers the risk of implant failure due to metal fatigue and mitigates the risk of cage subsidence.

This study differs from Zhang *et al.* in that it examines only two cage positions – anterior and posterior – while Zhang *et al.* analyze three: lateral, lateral-central, and anterior-central [14]. Zhang *et al.* found that the anterior-central cage position resulted in the lowest cage and screw stress, particularly under left rotation, compared to the lateral and lateral-central placements [14]. The current study, focusing on anterior and posterior positions, also highlights that anterior placement offers superior biomechanical stability, reducing stress on the implants. While Zhang *et al.* assessed a broader range of positions and movement modes, both studies agree that anterior cage positioning provides better load distribution and reduces the risk of subsidence.

In determining the screw diameter and length, the surgeon must rely primarily on measurements taken during surgery. The recommendations provided by this study serve as general guidelines; the suggested screw size and cage position are based on mechanical considerations for improving load distribution and stability. However, factors such as bone

quality, the shape and direction of the pedicle, the condition of the vertebral body, and the surgeon's experience are crucial in making the final decision. For instance, extending the screw too far towards the anterior cortex may increase the risk of bone perforation, particularly in patients with osteoporotic bone, which could potentially compromise nearby blood vessels. Therefore, while this analysis focuses on mechanical aspects, patient-specific characteristics must be considered during surgical planning to ensure both safety and effectiveness.

Despite the valuable insights provided by this study, there are several limitations to note. First, the thread-bone interface in the finite element model is treated as a bonded contact, which excludes small details related to the threads and the frictional interactions between the screw and the bone. This simplification is a common limitation in many current studies on spinal biomechanics. Second, the model does not differentiate between the cortical bone and cancellous bone, nor does it account for the posterior structures by assigning different modulus values to these components.

However, despite these limitations, the primary goal of this study remains to compare different configurations and identify which one provides better biomechanical performance in terms of stability and stress distribution. As such, the focus was less on achieving precise quantitative accuracy and more on understanding the general trend of biomechanical behavior under the various conditions. Future studies will aim to improve the model's accuracy by incorporating these considerations, thus enhancing the precision of the results.

4. CONCLUSIONS

The findings of this study highlight the significant impact of screw length and cage position on the biomechanics of TLIF constructs. The interbody cage used in this study has a banana-shaped structure and is made from PEEK, a biocompatible material known for its strength and durability in spinal fusion applications. Long screws with the screw tips extending beyond the fulcrum of the cage will increase the load-bearing capacity of the cage and reduce the stress on the connecting rod. In addition, anterior cage placement exhibits superior biomechanical properties compared to posterior position, as it reduces stress in the rod and on the L4 lower and L5 upper endplates. In contrast, when the cage is placed posteriorly, greater change in rod stress, especially during posture transitions, has been noticed and this is thought to be a risk factor of implant failure. Therefore, the results emphasize the importance of suitable screw length and cage positioning to improve the durability and stability of TLIF construction, with anterior cage placement and longer screws are more beneficial in terms of weight bearing and load distribution.

Acknowledgements. We acknowledge of Technology (HCMUT), VNU-HCM for supporting this study.

Credit authorship contribution statement. Le Duy Nguyen Ho: Investigation, Design model, Formal analysis, Manuscript preparation. Thi Hoang Thuy Le: Investigation, Design model, Formal analysis, Manuscript preparation. Thuc Tri Dang: Formal analysis, Review manuscript, Supervision. Truc Tam Vu: Conception, Formal analysis, Manuscript preparation, Supervision. Thien Tich Truong: Methodology, Review manuscript, Supervision.

Declaration of competing interest. The authors declare that they have no known competing financial interests or personal relationships that could have appeared to influence the work reported in this paper.

REFERENCES

1. Ozgur B. M., Yoo K., Rodriguez G., Taylor W. R. - Minimally-invasive technique for transforaminal lumbar interbody fusion (TLIF). Eur. Spine. J., **14**(9) (2005) 887-894. https://doi.org/10.1007/s00586-005-0941-3.
2. Mobbs R. J., Phan K., Malham G., Seex K., Rao P. J. - Lumbar interbody fusion: techniques, indications and comparison of interbody fusion options including PLIF, TLIF, MI-TLIF, OLIF/ATP, LLIF and ALIF. J. Spine Surg., **1**(1) (2015) 2-18.
3. Karikari I. O., Isaacs R. E. - Minimally invasive transforaminal lumbar interbody fusion: a review of techniques and outcomes. Spine, **35**(26S) (2010) S294-S301. https://doi.org/10.1097/BRS.0b013e3182022ddc.
4. Polly D. W., Jr., Klemme W. R., Cunningham B. W., Burnette J. B., Haggerty C. J., Oda I. - The biomechanical significance of anterior column support in a simulated single-level spinal fusion. J. Spinal Disord, **13**(1) (2000) 58-62. https://doi.org/10.1097/00002517-200002000-00012.
5. Materials A. Z. O. - Titanium Alloys - Physical Properties. https://www.azom.com/article.aspx?ArticleID=1341 (accessed 16 October 2024).
6. Materials A. Z. O. - Stainless Steel - Grade 304 (UNS S30400). https://www.azom.com/properties.aspx?ArticleID=965 (accessed 16 October 2024).
7. Materials A. Z. O. - Accelerated Ageing and Characterisation of UHMWPE used in Orthopaedic Implants. https://www.azom.com/properties.aspx?ArticleID=909 (accessed 16 October 2024).
8. Weisse B., Aiyangar A. K., Affolter C., Gander R., Terrasi G. P., Ploeg H. - Determination of the translational and rotational stiffnesses of an L4-L5 functional spinal unit using a specimen-specific finite element model. J. Mech. Behav. Biomed. Mater., **13** (2012) 45-61. https://doi.org/10.1016/j.jmbbm.2012.04.002.
9. Ahn Y. H., Chen W. M., Lee K. Y., Park K. W., Lee S. J. - Comparison of the load-sharing characteristics between pedicle-based dynamic and rigid rod devices. Biomed. Mater., **3**(4) (2008) 044101. https://doi.org/10.1088/1748-6041/3/4/044101.
10. Guo H. Z., Zhang S. C., Guo D. Q., Ma Y. H., Yuan K., Li Y. X., Peng J. C., Li J. L., Liang D., Tang Y. C. - Influence of cement-augmented pedicle screws with different volumes of polymethylmethacrylate in osteoporotic lumbar vertebrae over the adjacent segments: a 3D finite element analysis. BMC Musculoskelet. Disord., **21**(1) (2020) 460. https://doi.org/10.1186/s12891-020-03498-6.
11. Jiang R., Liu G. M., Bai H. T., Wang T. B., Wu H., Jia Y. Y., Luo Y. G. - Age-related differences in the biological parameters of vertebral cancellous bone from Chinese women. Chin. Med. J., **126**(20) (2013) 3828-3832. https://doi.org/10.3760/cma.j.issn.0366-6999.20131464.
12. Ulrich D., Van Rietbergen B., Laib A., Ruegsegger P. - The ability of three-dimensional structural indices to reflect mechanical aspects of trabecular bone. Bone, **25**(1) (1999) 55-60. https://doi.org/10.1016/S8756-3282(99)00098-8.
13. Kaleli N., Sarac D., Külünk S., Öztürk Ö. - Effect of different restorative crown and customized abutment materials on stress distribution in single implants and peripheral bone: A three-dimensional finite element analysis study. J. Prosthet. Dent., **119**(3) (2018) 437-445. https://doi.org/10.1016/j.prosdent.2017.03.008.
14. Zhang H., Hao D., Sun H., He S., Wang B., Hu H., Zhang Y. - Biomechanical effects of direction-changeable cage positions on lumbar spine: a finite element study. Am. J. Transl. Res., **12**(2) (2020) 389-396.